



A westerly wind dominated Puna Plateau during deposition of upper Pleistocene loessic sediments in the subtropical Andes, South America

Alex Pullen ^{1✉}, David L. Barbeau Jr², Andrew L. Leier², Jordan T. Abell ³, Madison Ward¹, Austin Bruner^{1,4} & Mary Kate Fidler¹

The Tafí del Valle depression (~27° S) in the eastern Andes of Argentina provides a record of late Pleistocene dust deposition in the subtropics of South America. We present large-*n* U-Pb geochronology data for detrital zircons from upper Pleistocene loess-paleosol deposits. When compared to regional data, the age spectra from the Tafí del Valle samples are most like the southern Puna Plateau, supporting derivation largely from the west and northwest. This runs counter to hypotheses suggesting these loessic sediments were derived from the low elevation plains to the east or extra-Andean Patagonia. Mapping of linear wind erosion features on the Puna Plateau yield a mean orientation of 125.7° (1 s.d. = 12.4°). These new data and existing records are consistent with a westerly-northwesterly dominated (upper- and lower-level) wind system over the southern Puna Plateau (to at least ~27° S) during periods of high dust accumulation in Tafí del Valle.

¹Department of Environmental Engineering and Earth Sciences, Clemson University, Clemson, SC 29634, USA. ²School of the Earth, Ocean and Environment, University of South Carolina, Columbia, SC 29208, USA. ³Department of Geosciences, University of Arizona, Tucson, AZ 85721, USA. ⁴Department of Geology, University of Kansas, Lawrence, KS 66045, USA. ✉email: apullen@clemson.edu

Determining the provenance of loess and loessic paleosols provides an opportunity to better understand ancient wind and precipitation patterns, surface conditions, and atmospheric dust loading which impacts the Earth's radiative forcing budget (e.g., ref. ¹). Once deposited, lithogenic dust influences biogeochemical processes in terrestrial and ocean environments (e.g., refs. ^{2–4}). Dust in the Southern Hemisphere is of particular importance because of the Southern Ocean's iron limitation on the productivity of photosynthetic organisms and disproportionate role in modulating Pleistocene climate (e.g., refs. ^{5,6}). A resolved understanding of Pleistocene dust production and transport in South America provides critical information about atmospheric circulation in the Southern Hemisphere and the nature of dust transported to the Southern Ocean and Antarctica during that interval.

The distribution of southern South America's Quaternary dust deposits have been well documented (e.g., ref. ⁷), and broadly include the southern Pampa loess⁸, the Chaco Plain loess⁹, eolian deposits of the northern Pampa—Río de la Plata region^{10,11} and smaller deposits in the eastern Andes (or pre-Andes; Fig. 1A, B)¹². Less certain, however, is the sediment provenance of these loess provinces, which is currently interpreted by competing models. Satellite data show that recent dust plumes originating from the

Altiplano–Puna Plateau generally track towards the southeast across the low elevation plains crossing locations with upper Pleistocene–Holocene loessic strata (Fig. 1A, B)¹³. But synoptic winds, lake levels, ice volumes, and precipitation were much different for long intervals during the late Pleistocene to early Holocene (e.g., ref. ¹⁴), making the practice of applying a post-industrial dust transport model to the paleoclimate problematic.

Similarities in bulk geochemistry between loess deposits along the eastern flank of the Andes with lower elevation loess deposits in the Pampean plains to the east led to the interpretation that the loess deposits along the eastern flank of the subtropical Andes were derived from the south¹⁵. In this scenario, late Pleistocene loess deposits along the eastern flank of the Andes are envisioned to mark the western edge of a dust source in the extra-Andean regions of Patagonia carried by southerly winds^{15,16}. Alternatively, provenance of the late Pleistocene loess deposits along the eastern flank of the Andes have also been attributed to the Chaco Plain, including parts of eastern Bolivia, western Paraguay, and northwest Argentina¹¹; this 'Chaco model' implicates northerly winds. Widely documented wind erosion of the southern Altiplano–Puna Plateau (e.g., refs. ^{17–21}) suggests that the loess deposits along the eastern flank of the Andes were largely sourced from the west and northwest, and that low elevation

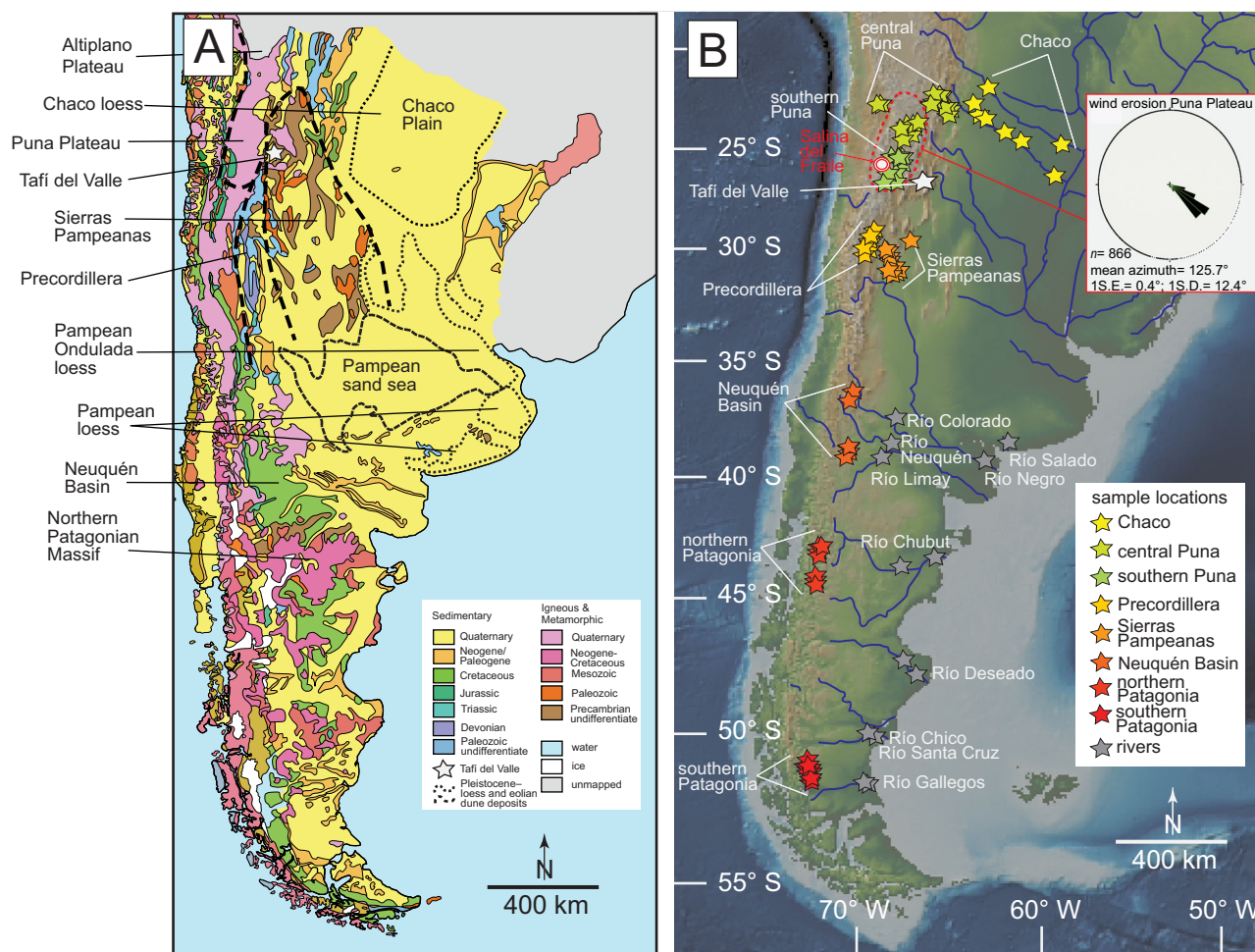


Fig. 1 Maps of southern South America. **A** Simplified geologic map of Argentina and central and southern Chile based on compilation maps^{54,55}. Distribution of La Pampa loess and Pampean Sand Sea after Iriondo (11,46) and Zárate (7). **B** Digital elevation model for southern portion of South America. Color filled stars denote locations of U–Pb zircon samples for comparison with Tafi del Valle samples: southern Puna Plateau^{37,38}, central Puna Plateau^{56–60}; Chaco^{36,61}; Sierras Pampeanas^{62–67}; Precordillera^{67–69}; Neuquén basin⁷⁰; northern Patagonia⁷¹; southern Patagonia⁷²; Ríos Neuquén, Salado, Limay, Colorado, Negro Chubut, Gallegos, Santa Cruz, Chico, and Deseado³⁶. Area of wind erosion study of Puna Plateau reported here highlighted by dashed red line; linear wind erosion data shown in inset rose plot.

plains of southern South America played a negligible role in the sourcing of this eolian detritus. Satellite based studies show the feasibility—at least under present-day-like climate conditions—of the Puna-Altiplano Plateau supplying dust to the eastern flank of the Andes and Chaco and Pampean plains to the east (e.g., refs. 13,22). Many modern dust events between 28°–37° S along the eastern flank of the Andes out to the Argentine plains result from short duration polar front outbreaks²³. These short duration shifts, on the order of several hours, most frequently occur in the austral autumn–winter months and result in westerly katabatic (referred to as Zonda) winds crossing the Andes and transporting dust towards the Argentine plains^{24,25}. Today, the core of the dust-carrying modern Zonda winds tends to be around 32° S²⁶.

Modern observations add to the ambiguity surrounding the provenance of the loess deposits along the eastern flank of the Andes. In addition to dust production within the high elevation Andes, present-day dust plumes originate at lower elevations (e.g., Mar Chiquita, a large saline lake in the central Argentine plains). These plumes indicate components of north- and south-directed atmospheric transport²⁷, further highlighting the uncertainty of southern South American loess provenance. This is particularly important considering the variability and differences between atmospheric circulation during the late Pleistocene and the present¹⁴. To better understand Quaternary dust provenance and wind erosion in southern South America and to help elucidate synoptic wind patterns during periods of dust accumulation over that time interval, we present new detrital-zircon geochronology data from an upper Pleistocene loess-paleosol succession near Tafi del Valle, Argentina, along with supporting wind erosion data from the Puna Plateau.

Geologic setting

Tafi del Valle is located at ~2200 m a.s.l. in a ~100 km² topographical depression in northwestern Argentina along the boundary between the arid southern Puna Plateau and semi-arid Chaco Plain (Fig. 1A, B). This area receives orographic precipitation when moisture-rich air of the South American low-level jet travels southward along the eastern slope of the Andes²⁸. Like other notable desert-fringing loess provinces such as the Chinese Loess Plateau and the Negev Desert, the Tafi del Valle loess has accumulated in an area along a steep precipitation gradient. Several exposures of laterally and vertically continuous interbedded loess and paleosol beds have been documented within the Tafi del Valle area^{12,15}. The Las Carreras section, studied here, contains a ~50 m thick stratigraphic section with 32 unique paleosol horizons interbedded with loess^{29,30} (Fig. 1B). The base of the Las Carreras section is assigned a minimum age of 1.15 Ma based on magnetostratigraphy²⁹; an age that is corroborated by optically-stimulated luminescence dating of a nearby 42-m loess-paleosol succession³¹. The age and number of interbedded loess and paleosol beds exposed in Las Carreras suggests a sub-100-ky orbital forcing signal on pedogenesis³⁰. The $N = 8$ loess and paleosol samples collected for this study range in age from ~6 ka to ~1.05 Ma based on the Schellenberger et al. (ref. 29) age model (Fig. 2). This sampling strategy was taken to sample strata presumably deposited around drier/cooler and wetter/warmer intervals in Tafi del Valle across the late Pleistocene and early Holocene.

The surface of the Puna Plateau to the west and northwest of the field area indicates extensive wind modification. Geomorphic features include yardangs, ventifacts, wind megaripples, and bedrock keeling ('wind tails'). Organization of gravel-mantled ripples on the Puna Plateau and linear erosional bedrock features indicate principally northwesterly geomorphically effective near-surface winds^{18,19,32} (Fig. 1; data presented herein). The southern

Puna Plateau includes up to 1.95 km of vertical wind deflation in the Salina del Fraile—approximately 250 km northwest of the Tafi del Valle field area—since the ~mid-Miocene²¹ (Fig. 1B).

The field area in Tafi del Valle (~27° S) is located beneath the northernmost position of the present-day subtropical westerly jet stream^{33,34}. During austral winter months, the subtropical jet shifts northward, such that the middle-to-upper tropospheric westerly winds move equatorward and further encompass Tafi del Valle³³ (Fig. 3). However, the interannual mean position of the lower-level Southern Hemisphere westerlies remains south of Tafi del Valle throughout the year with only periodic incursions (Fig. 3). This puts Tafi del Valle to the north of most sustained lower-level westerly wind activity, including Zonda winds, today.

Results

Linear wind erosion features on the southern Puna Plateau were mapped using composite satellite images to better understand the spatial distribution and orientations of these features with respect to the Tafi del Valle field area. These features include yardangs, wind streaks, and eolian modified interfluves (e.g., ref. 35). The $n = 866$ measurements yielded a mean orientation of 125.7° with low variability (1 s.d. = 12.4°; Fig. 1B; location and orientation of mapped elements are provided in Supplementary Table S1).

Detrital zircon geochronology was applied to Tafi del Valle deposits for its usefulness in assessing the provenance of highly mixed loessic sediments. The detrital zircon ages range from Pleistocene to Archean (Fig. 2A). The major age modes (and the range in percent of sample composition) are as follows: 0–23 Ma (6.5–11.8%); 450–650 Ma (38.5–50.0%), and 950–1200 Ma (20.5–40.7%; Supplementary Table S2; Table S3; Supplementary Fig. S1, S2). These major age modes also compose major components in potential source areas for the Las Carreras loess-paleosol sequence and are widely associated with the magmatic history of western South America³⁶. However, the major age modes along with minor age components can be recognized in different relative proportions by location through large-observation (large- n) data sets (Fig. 2A; S2) like those presented here ($n = 391$ –526).

Discussion

Comparison of the detrital zircon age spectra from Tafi del Valle with those of potential source areas inform the provenance of dust deposited in the subtropics along the eastern flank of the Andes during the late Pleistocene and early Holocene. In Fig. 2, we examine the age similarities and differences between the Tafi del Valle deposits and potential source areas along observed and proposed dust transport pathways (e.g., refs. 11,13,15). This is aimed at testing whether the upper Pleistocene and Holocene loessic deposits in Tafi del Valle were sourced from: (1) the lowlands of the Chaco Plain to the east¹¹, presumably when the Chaco was drier; (2) the extra-Andean areas of Patagonia (e.g., ref. 15), with possible storage of sediment in the Pampean plains; or (3) from the west-northwest on the Puna Plateau.

Zircon geochronology data from the southern Puna Plateau^{37,38} are most similar to data for individual and aggregate cumulative distributions of Tafi del Valle samples (Fig. 2A and Supplementary Fig. S1, S2). These similarities are supported by their locations in multi-dimensional scaling (MDS) space (Fig. 2B). We interpret this to mean that the southern Puna Plateau, to the west-northwest of the field area, contributed a large portion of the >20 μm detritus—20 μm being the analytical limit of the U-Pb measurements—to the upper Pleistocene and Holocene Tafi del Valle loess-paleosol strata. Considering the proximity of the southern Puna Plateau to Tafi del Valle, as well as the intervening high topography of the Eastern Cordillera

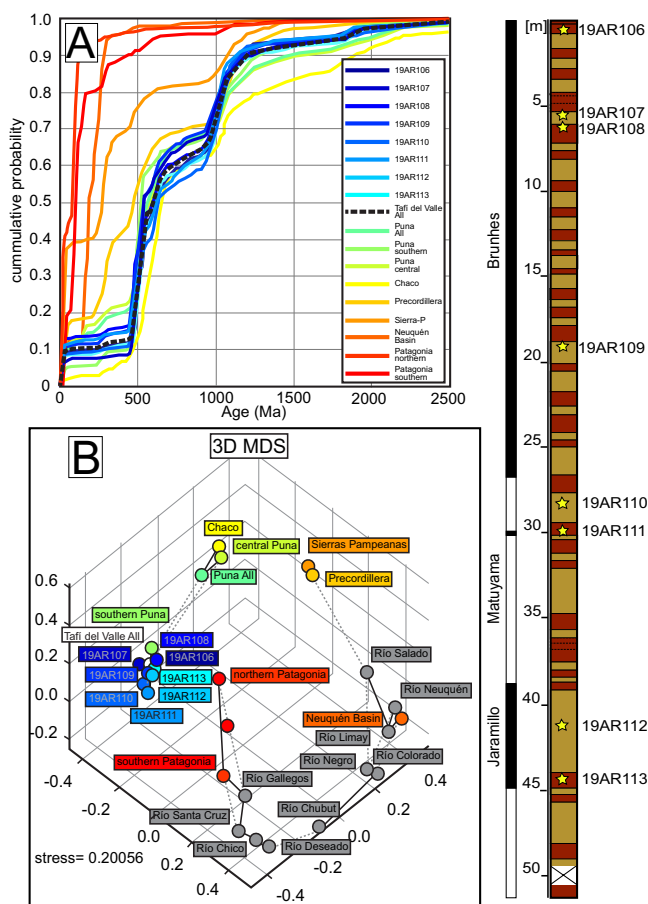


Fig. 2 U-Pb detrital zircon data. **A** U-Pb detrital zircon cumulative density functions for Tafi del Valle samples and comparison data. References for comparison data in the Fig. 1 caption with descriptions in Supplementary Table S2. **B** 3-dimensional multi-dimensional scaling (MDS) plot of U-Pb detrital zircon data for Tafi del Valle samples and comparison data. Measured and sampled stratigraphy, correlated with magnetostratigraphic timescale from Schellenbreger et al. (ref. 29); tan denotes loess and crimson denotes paleosol layers. 0 meters represents the top of the section and youngest strata.

between wind eroded areas of the Puna Plateau and Tafi del Valle, we speculate that most of the fine-grained fraction of detritus was likely sourced from this area as well. Rivers regionally sample bedrock, and river floodplains are often sources for desert-fringing loess deposits^{39,40}. To that end, in addition to using bedrock samples for detrital zircon age comparisons, we quantitatively compare our data with river samples from La Pampa and the extra-Andean Patagonia regions as a proxy for detrital zircon populations that could have been derived by winds to the south of Tafi del Valle (Fig. 2B, S1, S2). The detrital zircon data from the Sierra Pampeanas foreland, northern and southern Patagonian Andes—all areas south of Tafi del Valle—indicate poor quantitative similarities to the Tafi del Valle sediments (Fig. 2B). We interpret this to mean that most of the silt and larger fraction of detritus in the upper Pleistocene to Holocene Tafi del Valle loess-paleosol strata was not derived from southerly winds as previously proposed. Published data from the Chaco Plain is also a poor fit for the Tafi del Valle data, suggesting alternative wind orientations played a limited role in supplying the dust deposited in Tafi del Valle (Fig. 2B). Notably, the mobilization of Puna Plateau sediments within the westerly-northwesterly winds is consistent with inferences from bulk geochemical analysis of late Pleistocene dust sampled from the Antarctic ice sheet that largely

point to the Altiplano–Puna Plateau as a prominent proto-source for this dust⁴¹. Such a sediment routing pathway is also largely consistent with last glacial maximum (LGM) South American dust flux in general circulation models (e.g., ref. 42).

The high concentration of volcanic-derived particles in Tafi del Valle strata has been used to argue for a significant direct volcanic contribution to the loess-paleosol succession^{12,30}. However, only $n = 2$ detrital zircons (of $n = 4011$) in the Tafi del Valle samples yielded U-Pb ages that overlap (within uncertainty) the depositional ages of the respective samples. We interpret this to mean that direct volcanic contribution to the silt and larger fraction of the loess-paleosol strata was perhaps lower than previously thought—present but likely overwhelmed by the signal from older (e.g., Miocene) volcanic bedrock. Despite the absence of directly deposited volcanic zircons in our data, the percentage of detrital zircon with ages younger than 23 Ma is significant. This, coupled with observations of wind eroded volcanic deposits on the southern Puna Plateau, suggests substantial eolian reworking of Miocene and younger volcanic rocks.

Near surface wind orientations reconstructed from bedrock erosion features on the Puna Plateau and the volumetrically large wind deflation documented in areas like Salina del Fraile²¹ (Fig. 1B) could explain the abundance of loessic deposits along

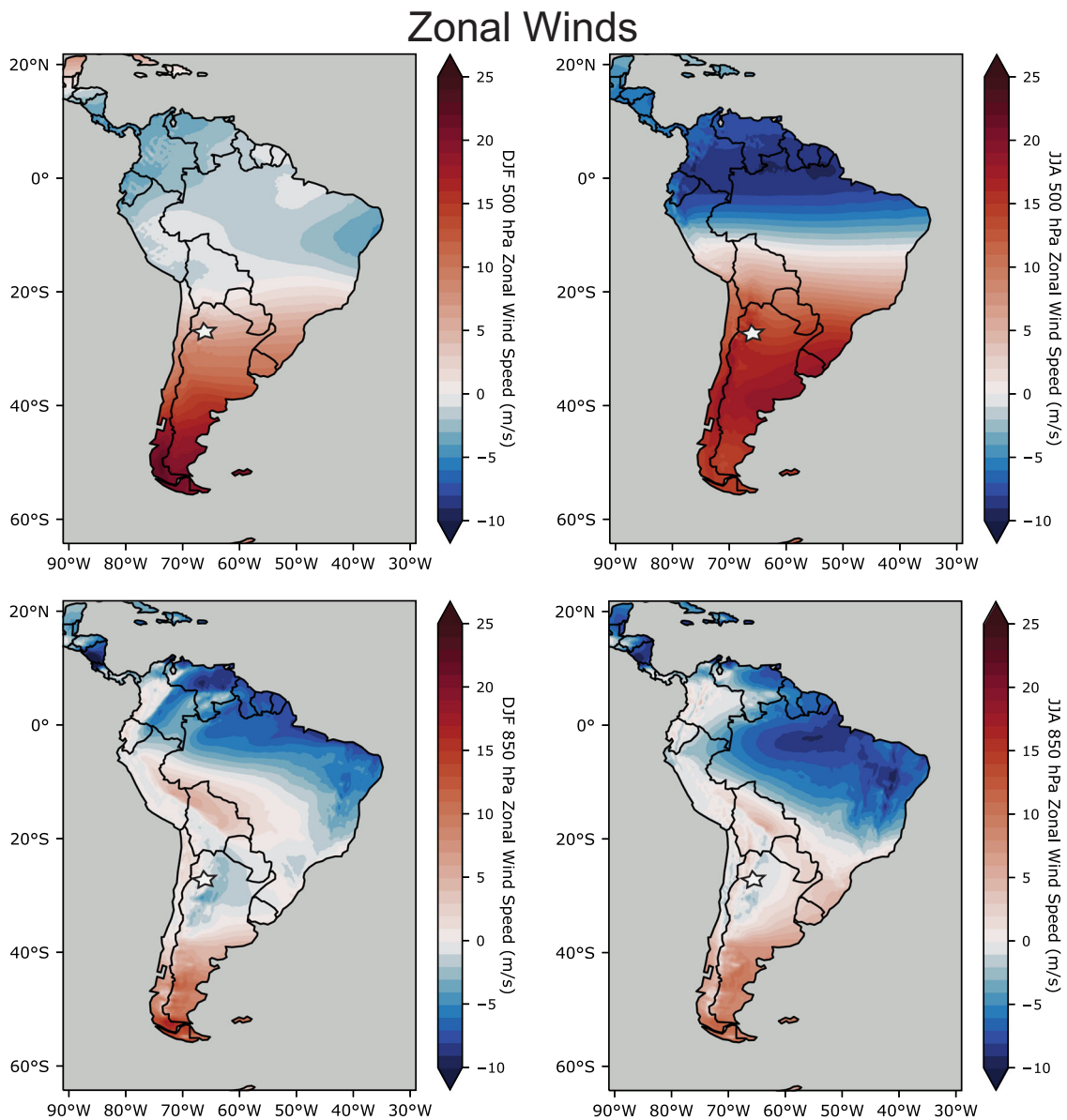


Fig. 3 The zonal components of wind at 500 hPa and 850 hPa for 1979–2021. Data from the ERA5 Reanalysis product⁷³. Positive values (red) denote westerly winds, whereas negative values (blue) denote easterly winds. The white star indicates the field location in Tafi del Valle.

the eastern flank of the subtropical Andes. Tafi del Valle, at least presently, is located along a steep precipitation gradient, but synoptic changes in moisture are needed to explain the interbedding of loess and paleosol strata.

In addition to evidence of westerly-northwesterly wind-supplied eolian sediment to the subtropical eastern Andes, the Tafi del Valle data do not indicate a significant shift in provenance throughout the stratigraphic section studied here at large-*n*. This observation is valuable for several reasons. (1) It implies little change to the sourcing of loessic sediment to Tafi del Valle across the Mid-Pleistocene Transition—an important change in the forcing of Earth’s glacial climate^{43,44}. (2) The lack of variability in detrital zircon provenance between loess and paleosol strata implies either little variation in sediment sourcing between dry and humid periods (assuming a relatively continuous accumulation of dust)—albeit with potentially different accumulation rates—or a preponderance of dust accumulation during drier periods with pedogenesis occurring during more humid intervals (as noted by ref. 30).

Presumably dust production in central and southern South America looked different throughout much of the late Pleistocene relative to present-day because of much different climatic and surficial conditions (e.g., ref. 14). This would include changes in wind intensity and position across spatial and temporal scales. Geomorphic evidence from the low elevation Pampean plains point toward important differences in near surface winds and surficial conditions during intervals of the late Pleistocene and early Holocene. Eolian dune fields of the Pampean Sand Sea were periodically active during the late Pleistocene and early Holocene but are mostly vegetation-stabilized at present⁴⁵. The Pampean Sand Sea covers $>2 \times 10^5$ km² (Fig. 1A)⁴⁶, which includes extensive low-amplitude (<10 m), longitudinal, kilometer-scale deflationary zones. Referred to as ‘las cubetas de deflación’, these deflationary depressions exhibit an anticlockwise pattern in satellite images across $>1 \times 10^5$ km² of the Pampean plains, retaining the geomorphically effective wind pattern that formed them, which may be a poor fit for present-day winds⁴⁷. A higher present-day water table compared to when the deflation depressions formed has

resulted in widespread shallow lakes across the Pampean plains, highlighting a lack of ongoing deflation. These geomorphic features in the Argentine lowlands are an indication of much different surface, moisture, synoptic wind, and dust production conditions during much of the late Pleistocene and early Holocene. To that end, applying a present-day-like dust model to South America for the Pleistocene would be imprudent.

Westerly-northwesterly winds supplied dust to Tafi del Valle during the late Pleistocene and early Holocene. But the nature of this westerly-northwesterly system(s) and the duration of its emplacement when dust was generated on the southern Puna and deposited in Tafi del Valle is uncertain. Paleoclimate data demonstrate that conditions in South America during the Pleistocene and Holocene were, for long intervals, much different than the present-day, with only brief periods approximating present-day-like conditions (e.g., ref. ¹⁴). A model aimed at explaining central South American dust dynamics across most of the late Pleistocene to early Holocene would need to consider not only the data presented here, but also explain (1) a < 100-ky periodicity in pedogenesis in Tafi del Valle, and (2) major differences between the present-day and late Pleistocene and early Holocene in the low elevation plains of southern South America to include large-scale eolian dune mobilization and deflation. To that end, we provide a brief discussion of the possible scenarios which could satisfy (most of) the available data.

Tafi del Valle is located at or slightly beyond the northern influence of present-day Zonda winds^{23,25} and within the dust generating influence of the Southern Hemisphere subtropical jet, particularly during the austral winter months. In a seminal study, Gaiero et al.¹³ utilized satellite data, a particle transport model, and geochemical analyses to suggest that dust storms in 2009 and 2010 originating from the Puna Plateau were associated with northward incursions of polar frontal systems, and experienced subsequent eastward transport related to the subtropical jet. While dust can be generated in this region year-round, today it is these short-term (hour- to day-long) events that drive substantial dust production. If this same concept was proposed for longer-term dust generation (i.e., the time interval covered by the geochemical data in this study), it would explain the uniformly westerly-northwesterly derived dust at Tafi del Valle, but it would be insufficient to explain the periodicity of loess accumulation and pedogenesis, which would have to be controlled by longer duration synoptic changes. Additionally, short-term displacements in zonal winds would not (alone) explain prolonged periods of greater-than-present aridity, wind erosion, and dust production in the Pampean plains.

Alternatively, longer-term, orbitally-forced processes may explain the loessic sediments and pedogenic cycles in Tafi del Valle, and provide a mechanism for changes in eolian transport and wind erosion at lower elevations in the Pampean plains. One possibility is that the frequency of the storm systems driving cold air advection to lower latitudes, and thus generating dust outbreaks on the Puna Plateau, varies temporally, which would be associated with changes in the jet streams and midlatitude westerlies⁴⁸. An additional mechanism could relate to a time-varied mean position of the Zonda winds, which today predominantly affect ~32–33° S²³, but have been suggested to shift with climate changes in the past (e.g., ref. ⁴⁹). These local features of atmospheric circulation are fundamentally connected to the subtropical jet stream and/or the midlatitude westerlies, and there is abundant evidence for variations in both of these systems at precessional (~19–23 ky), obliquity (~41 ky), and eccentricity (~100 ky) timescales across the Pleistocene and Holocene^{49–52}. Considering the new geochemical and geomorphologic data produced here, as well as existing records of pedogenesis, eolian activity, and hydrologic changes in nearby regions, we suggest

that longer-term displacements in synoptic winds likely need to be invoked to explain the provenance of the loessic strata in Tafi del Valle. We note that our records of dust provenance cannot distinguish the timescales of atmospheric circulation changes, but sub-eccentricity variability is likely present³⁰.

In summary, comparisons of U-Pb detrital zircon age spectra from upper Pleistocene loess and paleosol strata in the Tafi del Valle area of the Andean foothills with potential source areas indicate these crystals were sourced to the west and northwest on the Puna Plateau. This challenges previous assertions that the subtropical loess along the eastern flank of the Andes in South America was primarily sourced from extra-Andean Patagonia or the Chaco Plain. However, westerly-northwesterly derivation is consistent with extensive bedrock wind erosion on the Puna Plateau. If this provenance scenario is valid, it implies the emplacement of a westerly-northwesterly dominated wind system at ~27° S during periods of high dust accumulation at Tafi del Valle in the late Pleistocene and early Holocene.

Methods

Sampling and mineral separation. U-Pb detrital zircon samples were collected from the Las Carreras upper Pleistocene to Holocene section described in Schellenberger et al.²⁹ and Schellenberger and Veit³⁰. A handheld GPS and photos from Schellenberger and Veit³⁰ were used to confirm the location of the Las Carreras section. The field investigation and sample collection were completed with permission of the landowner. Samples were exported with permission of Argentine Customs Authority for academic use. Following the convention of Schellenberger and Veit³⁰, the section was measured from the stratigraphically youngest paleosol (S0) down to the base of the measured section. We used two investigators on the outcrop and one spotter to improve reproducibility of the stratigraphic measurement. $N = 8$ samples, weighing 2–3 kg each, were collected at 0.2 m (19AR106), 5.1 m (19AR107), 5.9 m (19AR108), 19 m (19AR109), 28.7 m (19AR110), 30.2 m (19AR111), 42 m (19AR112), and 43.2 m (19AR113) depth.

Zircon crystals were separated from the loess and paleosol samples using low hydraulic energies and ultrasonic disruption to minimize mineral separation induced grain-size age biases. Once the clay fraction was isolated from the zircon containing mineral fraction, methylene iodide was used to isolate the dense minerals. The zircon fraction was then isolated from the dense fraction using a barrier Frantz instrument. Aliquots of samples at different magnet settings were investigated under a reflected light microscope to check for the presence of zircon in the 'magnetic' fraction thus minimizing the introduction of mineral separation induced age bias. Zircon separates were homogenized and then poured onto double-sided tape to create 2.5 cm diameter cylindrical epoxy mounts for each sample. The epoxy zircon mounts were imaged using BSE on a Hitachi 3400 N SEM. These images were used to identify and avoid non-zircon on mounts and to avoid inclusions within zircon during LA-ICP-MS analysis.

Laser-ablation inductively-coupled-plasma mass-spectrometry. A Photon Analyte-G2 193 nm Excimer laser with a HelEx sample cell was used to ablate the detrital zircon crystals. Laser energy was set to 7 mJ. A He carrier gas was used to deliver analyte to the plasma. MFC1 was set to 0.10 l min⁻¹ and MFC2 was set to 0.30 l min⁻¹. A 3 burst 50 μm circular pre-ablation pass was used to clean sample surfaces and a 20 μm circular spot was used for analysis. Isotope ratios were measured on a Nu Instruments HR Multi-collection ICP-MS. Cool gas was set to 13.0 l min⁻¹, auxiliary gas to 0.80 l min⁻¹, and sample/make-up gas to 1.06 l min⁻¹. RF power was set to 1300 W. Faraday collectors were used to measure ²⁰⁶Pb, ²⁰⁷Pb, ²⁰⁸Pb, ²³²Th, ²³⁸U, whereas ²⁰²Hg and ²⁰⁴Pb + Hg were measured on ion counters. Isotope ratios were determined from a 6 s ablation window using a total counts method. Elemental and mass fractionation, initial-Pb correction, and instrument drift were corrected using the FC-1 and R33 zircon reference materials and the open-source data reduction AgeCalcML MATLAB code⁵³.

External uncertainties on ²⁰⁶Pb/²³⁸U for all samples ranged from 0.80% (2σ) to 0.38% (2σ), whereas the external uncertainties on ²⁰⁶Pb/²⁰⁷Pb ranged from 0.50% (2σ) to 0.36% (2σ). Following convention, the uncertainties shown below with the ages include only the internal uncertainties shown at 1σ. The 'Best Age' was assigned as ²⁰⁶Pb/²³⁸U age when the ²⁰⁶Pb/²³⁸U was <900 Ma, whereas the ²⁰⁶Pb/²⁰⁷Pb age was used when ²⁰⁶Pb/²³⁸U was >900 Ma. Ages >600 Ma with >20% discordance or >5% reverse discordance were not considered; as were dates with > ±10% internal uncertainty.

Geomorphic mapping. Linear wind erosion features were mapped on Landsat images in Google Earth (GE) Pro. Measurements between Landsat images in GE Pro were avoided to minimize errors induced from georegistration problems. Linear features were mapped as lines in GE Pro defining the long axis of the lineation. The geomorphic nature of linear features was determined through

analysis of landform geometry, size, local- and regional slope, and relief in GE. Geographic coordinates for the starting and ending positions of lines were converted to azimuth (°) in Excel.

Data availability

All new data generated in this study are available in the manuscript and supplementary material.

Received: 25 June 2021; Accepted: 6 June 2022;

Published online: 14 June 2022

References

- Kok, J. F., Ward, D. S., Mahowald, N. M. & Evan, A. T. Global and regional importance of the direct dust-climate feedback. *Nat. Commun.* **9**, 1–11 (2018).
- Vitousek, P. M. & Sanford, R. L. Jr Nutrient cycling in moist tropical forest. *Annu. Rev. Ecol. Syst.* **17**, 137–167 (1986).
- Yu, H. et al. The fertilizing role of African dust in the Amazon rainforest: A first multiyear assessment based on data from Cloud-Aerosol Lidar and Infrared Pathfinder Satellite Observations. *Geophys. Res. Lett.* **42**, 1984–1991 (2015).
- Tagliabue, A. et al. The integral role of iron in ocean biogeochemistry. *Nature* **543**, 51–59 (2017).
- Martin, J. H., Gordon, R. M. & Fitzwater, S. E. Iron in Antarctic waters. *Nature* **345**, 156 (1990).
- Moore, C. et al. Processes and patterns of oceanic nutrient limitation. *Nat. Geosci.* **6**, 701 (2013).
- Zárate, M. A. Loess of southern south America. *Quat. Sci. Rev.* **22**, 1987–2006 (2003).
- Zarate, M. & Blasi, A. Late Pleistocene and Holocene loess deposits of the southeastern Buenos Aires province, Argentina. *Geojournal* **24**, 211–220 (1991).
- Bertoldi de Pomar, H. Notas preliminares sobre la distribución de minerales edafógenos en la Provincia de Santa Fe. *Actas V Reunión Argentina de la Ciencia del Suelo, Santa Fe*, 716–726 (1969).
- González Bonorino, F. Mineralogía de las fracciones arcilla y limo del pampeano en el area de la Ciudad de Buenos Aires y su significado estratigráfico y sedimentológico. *Rev. de la Asociación Geológica Argent.* **20**, 67–148 (1965).
- Iriondo, M. H. Models of deposition of loess and loessoids in the Upper Quaternary of South America. *J. South Am. Earth Sci.* **10**, 71–79 (1997).
- Zinck, J. & Sayago, J. Loess–paleosol sequence of La Mesada in Tucuman province, northwest Argentina characterization and paleoenvironmental interpretation. *J. South Am. Earth Sci.* **12**, 293–310 (1999).
- Gaiero, D. M. et al. Ground/satellite observations and atmospheric modeling of dust storms originating in the high Puna-Altiplano deserts (South America): Implications for the interpretation of paleo-climatic archives. *J. Geophys. Res.: Atmospheres* **118**, 3817–3831 (2013).
- Kohfeld, K. et al. Southern Hemisphere westerly wind changes during the Last Glacial Maximum: paleo-data synthesis. *Quat. Sci. Rev.* **68**, 76–95 (2013).
- Sayago, J. M. The Argentine neotropical loess: an overview. *Quat. Sci. Rev.* **14**, 755–766 (1995).
- Sayago, J., Collantes, M., Karlson, A. & Sanabria, J. Genesis and distribution of the Late Pleistocene and Holocene loess of Argentina: a regional approximation. *Quat. Int.* **76**, 247–257 (2001).
- Inbar, M. & Risso, C. Holocene yardangs in volcanic terrains in the southern Andes, Argentina. *Earth Surf. Process. Landforms: J. Br. Geomorphological Res. Group* **26**, 657–666 (2001).
- Milana, J. P. Largest wind ripples on Earth? *Geology* **37**, 343–346 (2009).
- De Silva, S., Bailey, J., Mandt, K. & Viramonte, J. Yardangs in terrestrial ignimbrites: Synergistic remote and field observations on Earth with applications to Mars. *Planet. Space Sci.* **58**, 459–471 (2010).
- Hugenholtz, C. H., Barchyn, T. E. & Favaro, E. A. Formation of periodic bedrock ridges on Earth. *Aeolian Res.* **18**, 135–144 (2015).
- McMillan, M. & Schoenbohm, L. M. Large-scale cenozoic wind erosion in the puna plateau: the salina del fraile depression. *J. Geophys. Res.: Earth Surf.* **125**, e2020JF005682 (2020).
- Prospero, J. M., Ginoux, P., Torres, O., Nicholson, S. E. & Gill, T. E. Environmental characterization of global sources of atmospheric soil dust identified with the Nimbus 7 Total Ozone Mapping Spectrometer (TOMS) absorbing aerosol product. *Rev Geophys* **40** (2002).
- Norte, F. A. *Características del viento Zonda en la Región de Cuyo*, Universidad de Buenos Aires. Facultad de Ciencias Exactas y Naturales, (1988).
- Morrás, H. J. M. & Delaune, M. in *Congreso Argentino. 10. Latinoamericano de la Ciencia del Suelo. 8. 1983 10 23-28, 23 al 28 de octubre 1983.[Mar del Plata]*. AR.
- Norte, F. A. Understanding and forecasting Zonda wind (Andean foehn) in Argentina: a review. (2015).
- Norte, F. A., Ulke, A. G., Simonelli, S. C. & Viale, M. The severe zonda wind event of 11 July 2006 east of the Andes Cordillera (Argentina): a case study using the BRAMS model. *Meteorol. Atmos. Phys.* **102**, 1–14 (2008).
- Bucher, E. H. & Stein, A. F. Large salt dust storms follow a 30-year rainfall cycle in the Mar Chiquita Lake (Córdoba, Argentina). *PLoS One* **11**, e0156672 (2016).
- Vera, C. et al. The South American low-level jet experiment. *Bull. Am. Meteorological Soc.* **87**, 63–78 (2006).
- Schellenberger, A., Heller, F. & Veit, H. Magnetostratigraphy and magnetic susceptibility of the Las Carreras loess–paleosol sequence in Valle de Tafí, Tucumán, NW-Argentina. *Quat. Int.* **106**, 159–167 (2003).
- Schellenberger, A. & Veit, H. Pedostratigraphy and pedological and geochemical characterization of Las Carreras loess–paleosol sequence, Valle de Tafí, NW-Argentina. *Quat. Sci. Rev.* **25**, 811–831 (2006).
- Kemp, R. et al. Micromorphology and OSL dating of the basal part of the loess–paleosol sequence at La Mesada in Tucumán province, Northwest Argentina. *Quat. Int.* **106**, 111–117 (2003).
- Milana, J. P. & Kröhling, D. M. First data on volume and type of deflated sediment from Southern Puna Plateau and its role as source of the Chaco-Pampean loess. *Quat. Int.* **438**, 126–140 (2017).
- Garreaud, R. The Andes climate and weather. *Adv. Geosci.* **22**, 3–11 (2009).
- Garreaud, R., Vuille, M. & Clement, A. C. The climate of the Altiplano: observed current conditions and mechanisms of past changes. *Palaeogeogr., Palaeoclimatol., Palaeoecol.* **194**, 5–22 (2003).
- Perkins, J. P., Finnegan, N. J. & De Silva, S. L. Amplification of bedrock canyon incision by wind. *Nat. Geosci.* **8**, 305–310 (2015).
- Pepper, M. et al. Magmatic history and crustal genesis of western South America: Constraints from U–Pb ages and Hf isotopes of detrital zircons in modern rivers. *Geosphere* **12**, 1532–1555 (2016).
- Zhou, R., Schoenbohm, L. M., Sobel, E. R., Carrapa, B. & Davis, D. W. Sedimentary record of regional deformation and dynamics of the thick-skinned southern Puna Plateau, central Andes (26–27° S). *Earth Planet. Sci. Lett.* **433**, 317–325 (2016).
- Zhou, R., Schoenbohm, L. M., Sobel, E. R., Davis, D. W. & Glodny, J. New constraints on orogenic models of the southern Central Andean Plateau: Cenozoic basin evolution and bedrock exhumation. *Bulletin* **129**, 152–170 (2017).
- Enzel, Y. et al. The climatic and physiographic controls of the eastern Mediterranean over the late Pleistocene climates in the southern Levant and its neighboring deserts. *Glob. Planet. Change* **60**, 165–192 (2008).
- Nie, J. et al. Loess plateau storage of northeastern Tibetan plateau-derived Yellow River sediment. *Nat. Commun.* **6**, 8511 (2015).
- Gili, S. et al. Provenance of dust to Antarctica: A lead isotopic perspective. *Geophys. Res. Lett.* **43**, 2291–2298 (2016).
- Albani, S., Mahowald, N. M., Delmonte, B., Maggi, V. & Winckler, G. Comparing modeled and observed changes in mineral dust transport and deposition to Antarctica between the Last Glacial Maximum and current climates. *Clim. Dyn.* **38**, 1731–1755 (2012).
- Willeit, M., Ganopolski, A., Calov, R. & Brovkin, V. Mid-Pleistocene transition in glacial cycles explained by declining CO₂ and regolith removal. *Sci. Adv.* **5**, eaav7337 (2019).
- Berends, C., Köhler, P., Lourens, L. & van de Wal, R. (Wiley Online Library, 2021).
- Tripaldi, A. & Forman, S. L. Eolian depositional phases during the past 50 ka and inferred climate variability for the Pampean Sand Sea, western Pampas, Argentina. *Quat. Sci. Rev.* **139**, 77–93 (2016).
- Iriondo, M. The map of the South American plains. Its present state. *Quat. Sci. Am. Antarct. Penins* **6** (1990).
- Kruck, W. et al. Late pleistocene-holocene history of chaco-pampa sediments in Argentina and Paraguay. *EG Quat. Sci. J.* **60**, 188–202 (2011).
- Trenberth, K. E. Storm tracks in the Southern Hemisphere. *J. Atmos. Sci.* **48**, 2159–2178 (1991).
- Gili, S. et al. Glacial/interglacial changes of Southern Hemisphere wind circulation from the geochemistry of South American dust. *Earth Planet. Sci. Lett.* **469**, 98–109 (2017).
- Lamy, F. et al. Increased dust deposition in the Pacific Southern Ocean during glacial periods. *Science* **343**, 403–407 (2014).
- Lamy, F., Hebbeln, D., Röhl, U. & Wefer, G. Holocene rainfall variability in southern Chile: a marine record of latitudinal shifts of the Southern Westerlies. *Earth Planet. Sci. Lett.* **185**, 369–382 (2001).
- Lamy, F. et al. Precession modulation of the South Pacific westerly wind belt over the past million years. *Proc. Natl Acad. Sci.* **116**, 23455–23460 (2019).

53. Sundell, K. E., Gehrels, G. E. & Pecha, M. E. Rapid U-Pb geochronology by laser ablation multi-collector ICP-MS. *Geostand. Geoanalytical Res.* **45**, 37–57 (2021).
54. Gómez Tapias, J., Schobbenhaus, C. & Montes Ramírez, N. E. Geological map of south America. (2019).
55. SEGEMAR. (Secretaría de Industria Comercio y Minería de Argentina Buenos Aires, 1997).
56. Decelles, P. G., Carrapa, B. & Gehrels, G. E. Detrital zircon U-Pb ages provide provenance and chronostratigraphic information from Eocene synorogenic deposits in northwestern Argentina. *Geology* **35**, 323–326 (2007).
57. DeCelles, P. G. et al. The Miocene Arizaro Basin, central Andean hinterland: Response to partial lithosphere removal. *Geodynamics a Cordill. Orog. Syst.: Cent. Andes Argent. North. Chile.: Geol. Soc. Am. Mem.* **212**, 359–386 (2015).
58. Siks, B. C., Horton, B. K. Growth and fragmentation of the Andean foreland basin during eastward advance of fold-thrust deformation, Puna plateau and Eastern Cordillera, northern Argentina. *Tectonics* **30** (2011).
59. Henríquez, S., DeCelles, P. G. & Carrapa, B. Cretaceous to middle Cenozoic exhumation history of the Cordillera de Domeyko and Salar de Atacama basin, northern Chile. *Tectonics* **38**, 395–416 (2019).
60. Henríquez, S. et al. Deformation history of the Puna plateau, Central Andes of northwestern Argentina. *J. Struct. Geol.* **140**, 104133 (2020).
61. McGlue, M. M. et al. An integrated sedimentary systems analysis of the Río Bermejo (Argentina): megafan character in the overfilled Southern Chaco foreland basin. *J. Sediment. Res.* **86**, 1359–1377 (2016).
62. Adams, C., Miller, H., Aceñolaza, F., Toselli, A. & Griffin, W. The Pacific Gondwana margin in the late Neoproterozoic–early Paleozoic: Detrital zircon U-Pb ages from metasediments in northwest Argentina reveal their maximum age, provenance and tectonic setting. *Gondwana Res.* **19**, 71–83 (2011).
63. Fosdick, J. C., Carrapa, B. & Ortiz, G. Faulting and erosion in the Argentine Precordillera during changes in subduction regime: Reconciling bedrock cooling and detrital records. *Earth Planet. Sci. Lett.* **432**, 73–83 (2015).
64. Fosdick, J. C., Reat, E. J., Carrapa, B., Ortiz, G. & Alvarado, P. M. Retroarc basin reorganization and aridification during Paleogene uplift of the southern central Andes. *Tectonics* **36**, 493–514 (2017).
65. Reat, E. J. & Fosdick, J. C. Basin evolution during Cretaceous–Oligocene changes in sediment routing in the Eastern Precordillera, Argentina. *J. South Am. Earth Sci.* **84**, 422–443 (2018).
66. Capaldi, T. et al. Detrital zircon record of Phanerozoic magmatism in the southern Central Andes. *Geosphere* **17**, 876–897 (2021).
67. Capaldi, T. N. et al. Neogene retroarc foreland basin evolution, sediment provenance, and magmatism in response to flat slab subduction, western Argentina. *Tectonics* **39**, e2019TC005958 (2020).
68. Levina, M., Horton, B. K., Fuentes, F. & Stockli, D. F. Cenozoic sedimentation and exhumation of the foreland basin system preserved in the Precordillera thrust belt (31–32 S), southern central Andes, Argentina. *Tectonics* **33**, 1659–1680 (2014).
69. Capaldi, T. N., Horton, B. K., McKenzie, N. R., Stockli, D. F. & Odlum, M. L. Sediment provenance in contractional orogens: The detrital zircon record from modern rivers in the Andean fold-thrust belt and foreland basin of western Argentina. *Earth Planet. Sci. Lett.* **479**, 83–97 (2017).
70. Balgord, E. A. Triassic to Neogene evolution of the south-central Andean arc determined by detrital zircon U-Pb and Hf analysis of Neuquén Basin strata, central Argentina (34 S–40 S). *Lithosphere* **9**, 453–462 (2017).
71. Encinas, A. et al. Geochronologic and paleontologic evidence for a Pacific–Atlantic connection during the late Oligocene–early Miocene in the Patagonian Andes (43–44 S). *J. South Am. Earth Sci.* **55**, 1–18 (2014).
72. Leonard, J. S., Fosdick, J. C. & VanderLeest, R. A. Erosional and tectonic evolution of a retroarc orogenic wedge as revealed by sedimentary provenance: case of the Oligocene–Miocene Patagonian Andes. *Front. Earth Sci.* **7**, 353 (2020).
73. Hersbach, H. et al. ERA5 monthly averaged data on pressure levels from 1979 to present, Copernicus Climate Change Service (C3S) Climate Data Store (CDS). Accessed on (2019).

Acknowledgements

This research was funding the U.S. National Science Foundation (EAR–1911340 to A.P. and M.K.F. and EAR–1910510 to A.L.L. and D.L.B.). We thank Matthew Osman for assistance with the ERA5 wind data and three anonymous reviewers for their carefully constructed comments.

Author contributions

A.P., D.L.B., A.L.L., and M.K.F. designed the project. A.P., D.L.B., and A.B. conducted the field investigation and sample collection. A.P., D.L.B., A.B., and M.W. were responsible for data collection and synthesis. A.P., D.L.B., A.L.L., and J.T.A. made intellectual contributions to the manuscript.

Competing interests

The authors declare no competing interests.

Additional information

Supplementary information The online version contains supplementary material available at <https://doi.org/10.1038/s41467-022-31118-5>.

Correspondence and requests for materials should be addressed to Alex Pullen.

Peer review information *Nature Communications* thanks Chiara Költringer and the other, anonymous, reviewer(s) for their contribution to the peer review of this work.

Reprints and permission information is available at <http://www.nature.com/reprints>

Publisher's note Springer Nature remains neutral with regard to jurisdictional claims in published maps and institutional affiliations.



Open Access This article is licensed under a Creative Commons Attribution 4.0 International License, which permits use, sharing, adaptation, distribution and reproduction in any medium or format, as long as you give appropriate credit to the original author(s) and the source, provide a link to the Creative Commons license, and indicate if changes were made. The images or other third party material in this article are included in the article's Creative Commons license, unless indicated otherwise in a credit line to the material. If material is not included in the article's Creative Commons license and your intended use is not permitted by statutory regulation or exceeds the permitted use, you will need to obtain permission directly from the copyright holder. To view a copy of this license, visit <http://creativecommons.org/licenses/by/4.0/>.

© The Author(s) 2022